

Spectral characteristics of a gas saturated by a resonance field

V. A. Alekseev and T. L. Andreeva

P. N. Lebedev Physics Institute, USSR Academy of Sciences
(Submitted September 1, 1975)
Zh. Eksp. Teor. Fiz. 70, 1651-1659 (May 1976)

The shape of the nonlinear weak-wave absorption resonances in a gas in the presence of a strong field is considered for finite angles between the directions of propagation of the weak and strong waves. The possibility of using these resonances for scattered-light spectroscopy is discussed.

PACS numbers: 51.70.+f

1. INTRODUCTION

The methods of nonlinear spectroscopy allow us to obtain narrow resonances against a background of the relatively broad Doppler contour of the absorption line of atoms and molecules. At present these resonances are widely used to investigate the hyperfine structure of lines whose frequency coincides with a laser-transition frequency (see, for example, [1-5]).

In the present paper we propose to use a gas saturated by a resonance field as a spectral tool for investigating the spectra of scattered light. The essence of the method consists in the following. [6] A scattered-light signal $I_p(\omega)$ is applied to a cell containing an absorbing gas simultaneously with, and at a small angle θ to, a beam of laser radiation (of frequency ω_1) that saturates the cell. The scattered light is excited by another laser of the same type, but of frequency ω_2 . The frequency, ω_1 , of the laser illuminating the cell is tuned away from the frequency of the laser that causes the scattering within the limits of the Doppler line width $\Delta\omega_D$: $|\omega_2 - \omega_1| \leq \Delta\omega_D$. The scattered-light frequency region $|\omega - \omega_1| \leq \gamma$, where γ is the homogeneous line width of the gas, is transmitted by the cell better than the remaining part of the spectrum. Therefore, by tuning the frequency ω_1 away from the frequency of the scattering-inducing laser within the limits of the spectral width, $\Delta\omega_p$, of the scattered light, we can plot the entire scattering spectrum.

The intensity, J [photons/cm²-sec-sr], of the scattered light that is transmitted through the curvette with the absorbing gas is equal to

$$J(\omega) = \int I_p(\omega) \exp[-k(\omega)L] d\omega, \quad (1)$$

where L is the thickness of the curvette and $k(\omega)$ is the absorption coefficient of the gas saturated by the laser field:

$$k(\omega) = \alpha_l(\omega) [1 - \beta^2 f(\omega - \omega_1)]. \quad (2)$$

Here $\alpha_l(\omega)$ is the Doppler contour of the linear absorption of the gas, $\beta^2 f(\omega - \omega_1)$ describes the effect of the line saturation by the laser field, β^2 is the saturation parameter, which determines the contrast of the resonance, and $f(\omega - \omega_1)$ is the shape of the nonlinear resonance ($f(0) = 1$). The width, $\Delta\omega_f = \int f(\omega - \omega_1) d\omega$, of the

function $f(\omega)$ determines the resolving power of the method. Therefore, it is natural to assume that $\Delta\omega_f \ll \Delta\omega_p$. Assuming also that $\alpha_l L \lesssim 1$ and $\beta^2 \lesssim 1$, we obtain from (1) and (2) that

$$J(\omega) \approx J_b + J_u(\omega) = \int I_p(\omega) [1 - \alpha_l L] d\omega + I_p(\omega) \alpha_l(\omega) L \beta^2 \Delta\omega_f. \quad (3)$$

The signal from the photodetector registering the scattered light that has passed through the curvette, (3), contains two terms, the first of which determines the constant background J_b , while the second, $J_u(\omega)$, is the useful signal and is proportional to $I_p(\omega)$. The ratio, a , of the useful signal to the background is, in order of magnitude, equal to

$$a \approx \frac{\Delta\omega_f}{\Delta\omega} \alpha_l L \beta^2. \quad (4)$$

In our previous paper [6] we used the simplified expressions for the saturation parameter and the resonance shape:

$$\beta^2 = \left(\frac{dE}{\hbar} \right)^2 \frac{1}{\gamma\Gamma}, \quad f(\omega - \omega_1) = \frac{(2\gamma)^2}{(\omega - \omega_1)^2 + (2\gamma)^2}, \quad (5)$$

where E is the laser-wave field intensity, γ is the homogeneous line width, Γ is the population relaxation constant, d is the dipole moment of the transition, and \hbar is the Planck constant.

In the formula (5) it is assumed that the angle θ between the laser and scattered-light beams is equal to zero or is sufficiently small: $\theta \ll \gamma/\Delta\omega_D$. In a real situation we always have to deal with a whole set of values of the angle θ . Therefore, it is necessary to elucidate how the shape and contrast of the nonlinear absorption resonance change in the case of sufficiently large angles $\gamma/\Delta\omega_D \lesssim \theta \ll 1$.

Thus far, we have implied that the laser and scattered-light beams propagate in almost the same direction. In fact, we can also use the variant in which the laser and scattered-light beams propagate in almost opposite directions. It is not difficult to show that in this case the cell has a narrow transmission peak at the frequency $\omega = 2\omega_0 - \omega_1$, where ω_0 is the frequency of the atomic transition. In this variant it is, apparently, easier to separate the scattered light from the laser light.

The instrument function of the spectral device under consideration is determined by the shape of the nonlinear, weak-wave absorption resonance in the presence of a strong laser field. This problem was originally considered by Rautian^[7] with restrictions on the field and the relaxation constants of the operating levels. Subsequently, these limitations were removed in Baklanov and Chebotaev's papers,^[8] but the analysis was carried out for cases when the angle, θ , between the directions of propagation of the strong and weak waves is equal to zero or when $\theta = \pi$.

In the present paper the problem of the shape of the nonlinear, weak-wave absorption resonance in a gas in the presence of a strong wave is solved for the case of a finite angle, θ , between the directions of propagation of the interacting waves (Sec. 2). As will be seen from what follows, the angle θ is very important, and is, in a number of cases, the principal parameter determining the shape of the nonlinear resonance and the luminosity of the device.

In Sec. 3 we discuss the spectral characteristics of the absorbing cell, as well as the specific properties of atomic and molecular transitions in a gas. It turns out that the best characteristics are possessed by a cell with an atomic gas.

2. THE SHAPE OF THE WEAK-FIELD ABSORPTION LINE

Let us consider the shape of the absorption resonance for a weak wave in the presence of a strong laser field. We shall assume that on the cuvette with the absorbing gas are incident a strong laser field

$$\mathcal{E}_1 \exp [ik_1 R + i\omega_1 t] + \text{c.c.}$$

of wave vector \mathbf{k}_1 and frequency ω_1 and a weak wave

$$\mathcal{E}_2 \exp [ik_2 R + i\omega_2 t] + \text{c.c.}$$

of wave vector \mathbf{k}_2 and frequency ω_2 . The frequencies ω_1 and ω_2 are close to the transition frequency ω_0 of the absorbing gas. To describe the resonance interaction of the waves with the gas molecules, it is convenient to use the concept, introduced earlier in the papers^[9], of the density matrix $\sigma_{mn}(\mathbf{p}, \mathbf{p}')$, where m, n are quantum numbers of the electronic states of a molecule; and \mathbf{p}, \mathbf{p}' are the wave vectors of the motion of the center of inertia of the molecule. The system of equations for the density matrix was solved in third-order perturbation theory in the strong field \mathcal{E}_1 and in the linear approximation in the weak field \mathcal{E}_2 ,

Let us give the final expression for the coefficient, α [cm^{-1}], of absorption of the weak wave \mathcal{E}_2 in the case of almost parallel propagation of the waves \mathcal{E}_1 and \mathcal{E}_2 :

$$\alpha = \alpha_1 \left[1 - \left(\frac{d\mathcal{E}_1}{\hbar} \right)^2 \{C_1(\Omega) + C_2(\Omega)\} \right], \quad (6)$$

where α_1 is the standard Doppler contour of the linear absorption:

$$\alpha_1 = \frac{4\pi^2 d^2 \omega z_0}{\sqrt{\pi} k_2 v_0 c \hbar} \exp \left\{ - \left(\frac{\omega_2 - \omega_0}{k_2 v_0} \right)^2 \right\}, \quad (7)$$

$$C_1(\Omega) = \frac{2(\Gamma_1 + 2\gamma_v)}{\gamma_v(\Gamma_1 + \Gamma_2 + \gamma_v) \pi^2 \Delta k v_0} \text{Re} \int dx \frac{\exp \{-(x/\Delta k v_0)^2\}}{i(\Omega + x) + 2\gamma}, \quad (8)$$

$$C_2(\Omega) = \frac{4}{\sqrt{\pi} \Delta k v_0} \text{Re} \int dx \frac{1 + \Gamma_2/2 [i(\Omega + x) + \gamma_v]}{i(\Omega + x) + \Gamma_1 + \Gamma_2 + \gamma_v} \frac{\exp \{-(x/\Delta k v_0)^2\}}{i(\Omega + x) + 2\gamma}. \quad (9)$$

Here $d = d_{12} = d_{21}$ is the dipole moment of the transition, v_0 is the mean molecule velocity, z_0 is the averaged-over the velocities—difference between the populations of the levels 1 (the upper level) and 2 (the lower level) in the absence of the field, Γ_1 is the constant of the radiative decay from the level 1 to the level 2, while Γ_2 is the constant of the radiative decay from the level 1 to all the rest of the levels, γ_v is the impact-relaxation constant, $\gamma = (\Gamma_1 + \Gamma_2)/2 + \gamma_v$ is the transition-line width, $\Omega = \omega_2 - \omega_1$, and

$$|\Delta \mathbf{k}| = |\mathbf{k}_1 - \mathbf{k}_2| \approx k_2 \theta \ll k_1, k_2;$$

the direction of the vector $\Delta \mathbf{k}$ can be assumed to be perpendicular to the vector \mathbf{k}_2 . Notice that in the considered level scheme the lower level, 2, is the ground level and does not have a radiative decay channel. This scheme corresponds to the most realistic situation when, as the absorbing medium, we use an unexcited gas. For simplicity, the impact-relaxation constant γ_v is assumed to be the same for the upper and lower levels.

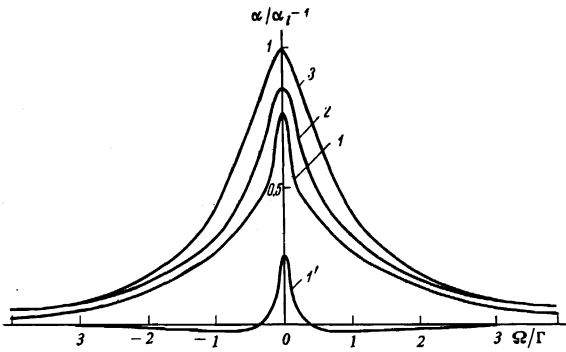
It can be seen from the formulas (6)–(9) that against the background of the Doppler linear-absorption contour α_1 are formed two narrow structures $C_1(\Omega)$ and $C_2(\Omega)$. The function $C_1(\Omega)$ is connected with the change, in the presence of the strong field, in the diagonal matrix elements $\sigma_{ii}(\mathbf{p}, \mathbf{p})$ and, therefore, describes the population depletion effect. The function $C_2(\Omega)$ is connected with the off-diagonal matrix elements $\sigma_{ii}(\mathbf{p}, \mathbf{p} + \mathbf{k}_1 - \mathbf{k}_2)$ and describes the influence on the absorption of the so-called nonlinear interference effect.^[8] A qualitative distinction of the spectral structures described by these functions can be seen from the fact that $\int C_2(\Omega) d\Omega = 0$, whereas

$$\int C_1(\Omega) d\Omega = \frac{2\pi(\Gamma_2 + 2\gamma_v)}{\gamma_v(\Gamma_1 + \Gamma_2 + \gamma_v)}. \quad (10)$$

The fact that the integral of the function $C_2(\Omega)$ is equal to zero, has been noted before by Baklanov and Chebotaev,^[8] who considered the $\theta = 0$ case, but without the use of perturbation theory in the strong field \mathcal{E}_1 . Apparently, this property has a general character, and does not depend on either the angles or the magnitude of the field.

The formulas (6)–(9) solve the problem of the shape of the absorption line for the weak signal \mathcal{E}_2 in the presence of the strong field \mathcal{E}_1 for an arbitrary relation between the relaxation constants $\Gamma_1, \Gamma_2, \gamma_v$ and the width $\Delta k v_0 = \Delta \omega_D \theta$, which is determined by the angle, θ , between the directions of propagation of the \mathcal{E}_1 and \mathcal{E}_2 waves.

Let us discuss the shape of the absorption line for dif-



The frequency dependence of the nonlinear part of the coefficient of absorption of the weak field: the curve 1) $\Gamma_1=0$, $\Gamma_2=\Gamma$, $\gamma_y/\Gamma=0.1$, $\beta_1^2=0.5$, $\beta_2^2=0.04$; the curve 1') is the plot of the function $(d^2/\hbar^2)C_2(\Omega)$ for the same values of the parameters as for the curve 1); curve 2) $\Gamma_1=0$, $\Gamma_2=\Gamma$, $\gamma_y/\Gamma=0.2$, $\beta_1^2=0.4$, $\beta_2^2=0.1$; curve 3) $\Gamma_2=0$, $\Gamma_1=\Gamma$, $\gamma_y/\Gamma=0.2$, $\beta_1^2=0.5$, $\beta_2^2=0.42$.

ferent relations between the width Δkv_0 and the relaxation constants. Let us first consider the simplest case of relatively large values of the angle θ , when $\Delta kv_0 \gg \gamma$, $\Gamma_1 + \Gamma_2$. In this case $C_2=0$ and, performing the integration in (8), we find for α the expression

$$\alpha = \alpha_1 [1 - \beta^2 f(\omega_1 - \omega_2)], \quad (11)$$

where

$$\beta^2 = \left(\frac{d\mathcal{E}_1}{\hbar} \right)^2 \frac{2\pi(\Gamma_2 + 2\gamma_y)}{\sqrt{\pi} \Delta kv_0 (\Gamma_1 + \Gamma_2 + \gamma_y) \gamma_y}, \quad (12)$$

$$f(\Omega) = \exp[-(\Omega/\Delta kv_0)^2], \quad \Delta\omega_f = \sqrt{\pi} \Delta kv_0.$$

As can be seen from (12), there arises against the background of the standard linear Doppler absorption-line contour α_1 , a dip of width $\sqrt{\pi} \Delta kv_0$.

In the opposite limiting case of small θ , when $\Delta kv_0 \ll \gamma$, we obtain for α the expression

$$\alpha = \alpha_1 [1 - \beta_1^2 f_1(\omega_1 - \omega_2) - \beta_2^2 f_2(\omega_1 - \omega_2)], \quad (13)$$

where

$$\begin{aligned} f_1(\Omega) &= \frac{4\gamma^2}{\Omega^2 + 4\gamma^2}, \quad \Delta\omega_f = 2\pi\gamma, \\ \beta_1^2 &= \left(\frac{d\mathcal{E}_1}{\hbar} \right)^2 \frac{\Gamma_2 + 2\gamma_y}{\gamma\gamma_y(\Gamma_1 + \Gamma_2 + \gamma_y)}; \\ f_2(\Omega) &= f_1(\Omega) \left\{ \frac{2\gamma(\Gamma_1 + \Gamma_2 + \gamma_y) - \Omega^2}{\Omega^2 + (\Gamma_1 + \Gamma_2 + \gamma_y)^2} \right. \\ &\quad \left. + \frac{\Gamma_2[2\gamma\gamma_y(\Gamma_1 + \Gamma_2 + \gamma_y) - \Omega^2(2\gamma + \Gamma_1 + \Gamma_2 + 2\gamma_y)]}{2(\Omega^2 + \gamma_y^2)[\Omega^2 + (\Gamma_1 + \Gamma_2 + \gamma_y)^2]} \right\}, \\ \beta_2^2 &= \left(\frac{d\mathcal{E}_1}{\hbar} \right)^2 \frac{1}{\gamma^2}, \quad \int f_2(\Omega) d\Omega = 0. \end{aligned} \quad (14)$$

For $\Gamma_1=0$ the expressions (13) and (14) coincide with the expressions obtained in^[8] for the $\theta=0$ case. The function $f_2(\Omega)$ has quite a complex spectral structure whose width may be smaller than the width of the function $f_1(\Omega)$. Thus, in the case when $\gamma_y \ll \Gamma_1 + \Gamma_2$ the function $f_2(\Omega)$ has a narrow resonance of width of the order of γ_y . The shape of the function $\alpha/\alpha_1 - 1$ for different relations between the parameters γ_y and $\Gamma_1 + \Gamma_2$ is shown in the figure.

We can consider in exactly the same fashion the case of oppositely directed laser and scattered-light waves, when

$$\mathbf{k}_1 = -\mathbf{k}_2, \quad \Delta\mathbf{k} = \mathbf{k}_1 + \mathbf{k}_2, \quad |\Delta\mathbf{k}| \approx k_2(\pi - \theta).$$

The absorption coefficient in this case has the form

$$\begin{aligned} \alpha &= \alpha_1 [1 - (d\mathcal{E}/\hbar)^2 C_1(\Omega)], \\ C_1(\Omega) &= \frac{2(\Gamma_2 + 2\gamma_y)}{\gamma_y(\Gamma_1 + \Gamma_2 + \gamma_y) \sqrt{\pi} \Delta kv_0} \operatorname{Re} \int dx \frac{\exp\{-i(x/\Delta kv_0)^2\}}{i(\Omega + 2\Delta\omega - x) + 2\gamma}, \quad (15) \\ \Delta\omega &= \omega_1 - \omega_0. \end{aligned}$$

Let us write out the explicit form of the absorption coefficient

$$\alpha = \alpha_1 [1 - \beta^2 f(\omega_1, \omega_2, \omega_0)]$$

in the case of large, $\Delta kv_0 \gg \gamma$, and small, $\Delta kv_0 \ll \gamma$, values of the angle $\pi - \theta$.

For $\Delta kv_0 \gg \gamma$ we have

$$\begin{aligned} f(\omega_1, \omega_2, \omega_0) &= \exp\left[-\left(\frac{\omega_1 + \omega_2 - 2\omega_0}{\Delta kv_0}\right)^2\right], \\ \Delta\omega_f &= \sqrt{\pi} \Delta kv_0 = \Delta\omega_D(\pi - \theta), \\ \beta^2 &= \left(\frac{d\mathcal{E}_1}{\hbar}\right)^2 \frac{2\pi(\Gamma_2 + 2\gamma_y)}{(\Gamma_1 + \Gamma_2 + \gamma_y) \gamma_y \sqrt{\pi} \Delta kv_0}. \end{aligned} \quad (16)$$

For $\Delta kv_0 \ll \gamma$ we obtain

$$\begin{aligned} f(\omega_1, \omega_2, \omega_0) &= \frac{4\gamma^2}{(\omega_1 + \omega_2 - 2\omega_0)^2 + 4\gamma^2}, \quad \Delta\omega_f = 2\pi\gamma, \\ \beta^2 &= \left(\frac{d\mathcal{E}_1}{\hbar}\right)^2 \frac{2(\Gamma_2 + 2\gamma_y)}{\gamma\gamma_y(\Gamma_1 + \Gamma_2 + \gamma_y)}. \end{aligned} \quad (17)$$

As can be seen from the formulas (16) and (17), the difference between this case and the case of unidirectional waves consists in the fact that the transmission resonance arises now at the frequency $\omega_2 = \omega_0 + (\omega_0 - \omega_1)$, which is tuned away from the line center ω_0 by the value $\omega_0 - \omega_1$. Let us recall that in the case of almost parallel laser and scattered-light waves the resonance appears at the frequency $\omega_2 = \omega_1$, and that its position does not depend on the transition eigenfrequency ω_0 .

3. THE SPECTRAL CHARACTERISTICS OF THE ILLUMINATED CELL

The above-considered variant of the gas cell illuminated by a laser field is essentially a fairly narrow-band filter whose transmission band of width $\Delta\omega$, $\approx 10^4 - 10^7$ Hz can be retuned within the limits of the Doppler line width of the working gas of the cell (in the visible region of the spectrum this spectral band is $\sim (5 - 15) \times 10^8$ Hz). In case of need this band can be further broadened several times with the aid of an external magnetic field.

The only spectral instrument that has a resolving power $\Delta\omega_f \sim 10^6 - 10^7$ Hz is the Fabry-Perot interferometer, the resolutions region $\Delta\omega_f \approx 10^6$ Hz being in practice extremely difficult to realize.^[10] As will be seen from what follows, the illuminated cell as a spectral instrument possesses a much greater liminosity than

the Fabry-Perot interferometer for the same resolutions. Furthermore, the resolving power of the cell can, in principle, be improved right up to values $\Delta\omega_f \approx 10^4 - 10^5$ Hz, which, for the interferometer, are generally unattainable. The saturated—by a laser field—cell can be used in two ways. In the first case the scattered-light beam under investigation is directed at the cell at a small angle θ to the illuminating laser beam. In the second case the scattered light falls on the cuvette in a direction almost opposite to that of the laser beam. The resolving powers of the method in the two cases are virtually equal (see Sec. 2), but there appears a difference in the contrast of the transmission peak of the cell.

Let us begin the consideration of the spectral characteristics of the cell with the variant of almost parallel propagation of the laser and scattered-light beams.

For practical use the case of the sufficiently narrow instrument function, when $\Delta\omega_f \ll \Delta\omega_D$, is of greatest interest. Then the observable magnitude, $J_u(\omega_1)$, of the useful scattered-light signal transmitted through the cuvette (see (3)) is proportional to the integral of the instrument function over the frequencies, i. e.,

$$J_u(\omega_1) \propto \int C_1(\Omega) d\Omega + \int C_2(\Omega) d\Omega$$

(see (6)–(8)). As has already been noted above, $\int C_2(\Omega) \times d\Omega = 0$, and, therefore, the function $C_2(\Omega)$ in the case under consideration does not, in general, contribute to the spectral characteristics of the illuminated cell. The integral of the function $C_1(\Omega)$ is determined by the formula (10). Substituting (10) into (1) and (2), we obtain for the quantity $J_u(\omega_1)$ [photons/cm²-sec-sr] the expression

$$J_u(\omega_1) = I_p(\omega_1) \left(\frac{d\beta_1}{h} \right)^2 \frac{2\pi(\Gamma_1 + 2\gamma_u)}{\gamma_u(\Gamma_1 + \Gamma_2 + \gamma_u)} \alpha_1 L, \quad (3a)$$

$$a = 2\pi\gamma\alpha_1 L \beta_1^2 / \Delta\omega_D, \quad \beta_1^2 \ll 1. \quad (4a)$$

As can be seen from the expression (3a), the magnitude of the useful signal depends quite weakly on the gas density N in the absorbing cell. Since $\alpha_1 \propto N$ and $\gamma_u \propto N$, the quantity $J_u(\omega_1)$ does not depend on the density at low N ($\gamma_u \ll \Gamma_2$) and at high N ($\gamma_u \gg \Gamma_1, \Gamma_2$), changing as we go over from low to high densities by only a factor of two.

The resolving power, $\Delta\omega_f$, of the illuminated cell is determined by the maximum of the quantities $\Delta\omega_f = \max[\gamma, \Delta\omega_D\theta]$, which in the case under consideration is much smaller than the width of the scattered-light spectrum: $\max[\gamma, \Delta\omega_D\theta] \ll \Delta\omega_D$. Therefore, the angle θ is limited by the condition

$$\theta \ll \Delta\omega_f / \Delta\omega_D. \quad (18)$$

It is worth noting that the instrument function of the device has different forms in the cases $\theta \ll \gamma / \Delta\omega_D$ (see (13)) and $\gamma / \Delta\omega_D \ll \theta \ll \Delta\omega_f / \Delta\omega_D$ (see (12)). However, the integral of the instrument function has one and the same value (3a) in the entire region of θ values defined by the inequality (18). The limiting value of the re-

solving power of the cell is determined by the probability, $\Gamma_1 + \Gamma_2$, of the radiative decay of the upper operating level, and is attained at angles $\theta \lesssim (\Gamma_1 + \Gamma_2) / \Delta\omega_D$. Thus, the resolving power of the cell can be varied within the broad range from γ to $\Delta\omega_D\theta$.

Let us now compare the liminosity of the illuminated absorbing cell with the luminosity of the Fabry-Perot interferometer.¹⁾ The luminosity, ΔO_i , of the interferometer (see, for example,^[11]) is determined only by the resolving power of the interferometer, and is equal to $\Delta O_i = \theta_i^2 = 2\Gamma/\omega$, where θ_i is the permissible angle of inclination of the beam to the axis of the plane-parallel interferometer, Γ is the halfwidth of the transmission band, and ω is the frequency of the light.

The luminosity of the illuminated cell, ΔO , is also determined by its resolving power $\Delta\omega_f = \Delta\omega_D\theta$: $\Delta O = \theta^2 = (\Delta\omega_f / \Delta\omega_D)^2$. For the same resolving powers, i. e., for $\Gamma = \Delta\omega_f$, the ratio of the luminosity of the cell to the luminosity of the interferometer is

$$\frac{\Delta O}{\Delta O_i} = \frac{1}{2} \frac{\omega \Delta\omega_f}{\Delta\omega_D^2}. \quad (19)$$

For visible light of frequency $\omega \approx \frac{1}{2} \times 10^{15}$ Hz and $\Delta\omega_D \approx 5 \times 10^8$ Hz we obtain $\Delta O / \Delta O_i \approx 10^{-3} \Delta\omega_f$ [Hz]. As the value of $\Delta\omega_f$ is varied from 10^5 to 10^8 Hz the ratio $\Delta O / \Delta O_i$ varies within the range from 10^2 to 10^5 . Notice that the resolution region $\Gamma \approx 10^6$ Hz is a difficult region for the investigation of scattering spectra with the aid of the Fabry-Perot interferometer, as well as by the optical-shift methods, which are best in the region $\Delta\omega_f \lesssim 10^5$ Hz.^[10,11] Therefore, in the resolution region $\sim 10^6 - 10^8$ Hz the illuminated cell may prove to be the most convenient spectral instrument for investigating light scattering.

In the case of oppositely-directed laser and scattered-light signals all the results pertaining to the resolving power and the luminosity of the method remain the same, but the contrast may decrease in comparison with (4a) because of the presence of a hyperfine structure of the line inside the Doppler contour. As can be seen from the formulas (16) and (17), in this case a transmission peak arises at the frequency $\omega_2 = 2\omega_{0i} - \omega_1$, where ω_{0i} is the frequency of the i -th component of the hyperfine structure. The remaining components of the hyperfine structure (for example, in the case of J_2 ^[13,14] the number of components $m \sim 20$) produce at the frequency ω_2 a background whose intensity is proportional to the number m . Therefore, there arise m transmission peaks against the background of the linear absorption coefficient, but the contrast of each peak $\sim \beta_1^2 / m$, i. e., it decreases m times in comparison with the single line or with the variant of unidirectional waves.

As can be seen from the formula (4a), the ratio of the useful signal to the background cannot, even under optimal experimental conditions, when $\alpha_1 L \approx 1$ and $\beta_1^2 \approx 1$, be greater than the value $a = 2\pi\gamma / \Delta\omega_D < 1$, i. e., in the method under consideration the useful signal is always smaller than the background. Furthermore, in detecting the signal it is necessary to separate the scattered light from the laser signal illuminating the cell. A

purely geometrical separation of the beams is the simplest to achieve in the variant of oppositely directed waves. In the case of parallel propagation of the beams, a geometrical separation of them is also possible, since the laser light has virtually a diffractive divergence, while the scattered light propagates in quite a wide solid angle $\theta^2 \approx (\Delta\omega_p/\Delta\omega_D)^2$. For a more precise separation we can also use the methods of polarization decoupling and the method of synchronous detection.

The last method is widely used at present in nonlinear spectroscopy.^[13,14] Here the illuminating laser beam is modulated by a low frequency $\Omega \sim 500 - 100$ Hz, and the Ω component is separated out by the method of synchronous detection in a weak scanning beam. In our case it is convenient to modulate both signals—the laser beam with frequency Ω_1 and the scattered-light signal with frequency Ω_2 . The intensities of the laser light, I_1 , and the scattered light, I_p , are equal to

$$I_1 = I_1^{(0)} \frac{1 + \cos \Omega_1 t}{2}, \quad I_p = I_p^{(0)} \frac{1 + \cos \Omega_2 t}{2},$$

while the $\Omega_1 + \Omega_2$ component of the signal from the photodetector registering the scattered light has the form

$$J(\omega_1, \Omega_1 + \Omega_2) = \frac{1}{2} I_p^{(0)}(\omega_1) \alpha_l L \beta^2 \Delta\omega_l.$$

The signal from the photodetector does not contain a background at the frequency $\Omega_1 + \Omega_2$. Synchronous detection also eliminates exactly the cell's harmful spontaneous-emission signal, which turns out to be modulated, just like the laser light, at the frequency Ω_1 .

It follows from the foregoing that the most important gas parameters in a luminous cell are the following: 1) the radiative-decay probability $\Gamma = \Gamma_1 + \Gamma_2$, which determines the maximum attainable resolving power of the method; 2) the value of the power W_s [W/cm²] of the laser field necessary for the saturation of the operating transition of the gas; 3) the magnitude of the linear absorption coefficient of the working gas.

It is well known that the frequencies of the electronic vibrational-rotational transitions of molecular iodine in the visible region of the spectrum coincide with the frequencies of the radiation of the most widely used Ar⁺ and He-Ne lasers.^[12-15] However, for scattered-light spectroscopy these transitions are, apparently, inconvenient. In this case the radiative decay of the upper state occurs simultaneously along many channels corresponding to transitions to a large number of vibrational levels of the lower electronic term; therefore, $\Gamma_2 \gg \Gamma_1$. As a result, the saturating-power value, which is determined by the value of Γ_2 , turns out to be very large: $W_s \approx 1 - 10$ W/cm²,^[5,13,14] while the linear absorption coefficient, determined by the quantity Γ_1 , turns out to be small: $\alpha_l \approx 0.02$ cm⁻¹-Torr⁻¹.^[15] This situation is, apparently, typical of all electronic transitions in molecular spectra.

It is most convenient to use a cell with an atomic gas having in the visible region of the spectrum absorption lines corresponding to transitions from the ground

state. Here we have in mind the use of tunable—with the aid of dyes—Ar⁺-laser systems that have now been developed. It is desirable that the probability, Γ_1 , of the radiative decay of the upper state be sufficiently small: $\Gamma_1 \approx 10^4 - 10^6$ Hz. These requirements are satisfied, in particular, by the intercombination transitions of the elements of the second group, for example, in Sr by the transition $^1S_0 - ^3P_1$, $\lambda = 689$ nm, $\Gamma_1 \approx 10^4$ Hz and in Ba by the transition $^1S_0 - ^3P_1$, $\lambda = 791$ nm, $\Gamma_1 \approx 5 \times 10^5$ Hz.^[16] For these transitions the lower 1S_0 state does not have a hyperfine splitting, and, therefore, the quantity $\Gamma_2 = 0$. The coefficient of linear absorption attains a value $\alpha = 1$ cm⁻¹ in the case of Sr at a density $N \approx 10^{14}$ cm⁻³ and in the case of Ba at $N \approx 10^{12}$ cm⁻³. The condition that $\alpha_l L \approx 1$ for atomic gases is easily fulfilled for a cuvette length $L \approx 1$ cm and at sufficiently low densities $N \lesssim 10^{14}$ cm⁻³. The laser-field power W_s necessary for the brightening of a cell with an atomic gas turns out to be several orders of magnitude smaller than the corresponding value for a molecular gas. For the $\lambda = 689$ -nm Sr transition, setting $N \approx 10^{14}$ cm⁻³, the quantity $\gamma_y \approx 3 \times 10^4$ Hz at this density²⁾, and $\Delta\omega_D \theta = 10^6$ Hz, we obtain for the saturating power $W_s \approx 4 \times 10^{-5}$ W/cm². For the $\lambda = 791$ -nm Ba transition in the case when $N = 10^{12}$ cm⁻³, the value of $\gamma_y \approx 3 \times 10^2$ Hz $\ll \Gamma_1$. Taking into account the fact that $\Delta\omega_D \theta \approx 10^6$ Hz, we obtain for the saturating power $W_s \approx 6 \times 10^{-6}$ W/cm².

Another advantage of an atomic gas consists in the fact that in this case we can use the variant of oppositely directed laser and scattered-light beams. It is then by far easier to geometrically separate the laser and scattered-light beams. In contrast to a molecular gas, the splitting of the hyperfine structure of the considered Ba and Sr transitions is greater than the Doppler line width and, therefore, does not lead to a reduction in the contrast of the method.

The authors are grateful to B. Ya. Zel'dovich and I. I. Sobel'man for valuable discussions.

¹⁾As is well known, the Fabry-Perot interferometer has a higher luminosity than any other spectral device.^[12]

²⁾We have in mind in estimating the values of γ_y typical line-width values $\sim 10^7$ Hz/Torr for the van der Waals broadening mechanism. The broadening due to the resonance transfer of excitation for the considered transitions is of the same order of magnitude.

¹W. E. Lamb, Phys. Rev. 134A, 1429 (1964).

²N. G. Basov and V. S. Letokhov, Pis'ma Zh. Eksp. Teor. Fiz. 2, 6 (1966) [JETP Lett. 2, 3 (1965)].

³R. L. Barger and J. L. Hall, Phys. Rev. Lett. 22, 4 (1969).

⁴N. G. Basov, O. N. Kompanets, V. S. Letokhov, and V. V. Nikitin, Zh. Eksp. Teor. Fiz. 59, 394 (1970) [Sov. Phys. JETP 32, 214 (1971)].

⁵M. D. Levenson and A. L. Schawlow, Phys. Rev. A6, 10 (1972).

⁶V. A. Alekseev and T. L. Andreeva, Pis'ma Zh. Eksp. Teor. Fiz. 20, 316 (1974) [JETP Lett. 20, 140 (1974)].

⁷S. G. Rautian, Trudy FIAN, Vol. 43, Nauka, 1968, pp. 3-113.

⁸E. V. Baklanov and V. P. Chebotayev, Zh. Eksp. Teor. Fiz. 60, 552 (1971); 61, 922 (1971) [Sov. Phys. JETP 33, 300 (1971); 34, 490 (1972)].

⁹V. A. Alekseev, T. L. Andreeva, and I. I. Sobel'man, Zh.

- Eksp. Teor. Fiz. 62, 614 (1972); 64, 813 (1973) [Sov. Phys. JETP 35, 325 (1972); 37, 413 (1973)].
- ¹⁰Physical Acoustics (ed. by W. Mason and R. Thurston), Vol. 6, Academic Press, New York, 1970 (Russ. Transl., Mir, 1973).
- ¹¹V. A. Alekseev, B. Ya. Zel'dovich, and I. I. Sobel'man, *Kvantovaya Elektron. (Moscow)* 2, 1007 (1975) [Sov. J. Quantum Electron. 5, 547 (1975)].
- ¹²P. Jacquinot, *J. Opt. Soc. Am.* 44, 761 (1954).
- ¹³W. G. Schweitzer, Jr., E. G. Kessler, Jr., R. D. Deslattes, H. P. Layer, and J. R. Whetstone, *Appl. Opt.* 12, 2927 (1973).
- ¹⁴M. S. Sorem and A. L. Schawlow, *Opt. Commun.* 5, 148 (1972).
- ¹⁵G. R. Hanes, J. Lapierre, P. R. Bunker, and K. C. Shotton, *J. Mol. Spectrosc.* 39, 506 (1971).
- ¹⁶S. É. Frish, *Opticheskie spektry atomov (Optical Spectra of Atoms)*, Nauka, 1963.

Translated by A. K. Ageyi

Selective two-step ionization of rubidium by laser radiation

R. V. Ambartsumyan, A. M. Apatin, V. S. Letokhov, A. A. Makarov,
V. I. Mishin, A. A. Puretskii, and N. P. Furzikov

Institute of Spectroscopy, USSR Academy of Sciences
(Submitted September 13, 1975)
Zh. Eksp. Teor. Fiz. 70, 1660-1673 (May 1976)

Selective application of pulsed laser radiation from dye and ruby lasers was used to produce two-step ionization of rubidium atoms with initial ion density of about 10^{13} cm^{-3} per pulse. Every excited atom of rubidium was ionized, i.e., radiation-intensity saturation was achieved for the second step. The yield of ions as a function of the exciting and ionizing intensities and of the density of atoms was investigated both experimentally and theoretically. This analysis was used as a basis for a simple method of measuring the photoionization cross sections for atoms in excited states, which did not require a knowledge of the absolute number of excited atoms. The method was used to measure the cross sections for photoionization from the 6^2P state of the Rb atom by fundamental-frequency radiation from a ruby laser [$\sigma_2 = (1.7 \pm 0.3) \times 10^{-17} \text{ cm}^2$] and the second-harmonic radiation from a ruby laser [$\sigma_2 = (0.19 \pm 0.03) \times 10^{-17} \text{ cm}^2$].

PACS numbers: 32.10.Qy

1. INTRODUCTION

The exceedingly small spectral width of a laser line makes the laser a very precise instrument for the selective interaction with matter, and the high intensity of laser radiation ensures that this interaction occurs very efficiently. Two-step ionization is one of the most universal methods of selective interaction between laser radiation and atoms and molecules. It was first proposed and used in^[1,2]. Its principle is as follows. Laser radiation at frequency ν_1 is absorbed by atoms of a selected type (for example, atoms of the required isotopic composition or those containing nuclei of a particular isomer, or simply atoms of a particular element), and transitions to the excited state take place. A second laser operating at frequency ν_2 is then used to ionize the selectively excited atoms, and this second frequency is chosen so that atoms still in the ground state are not ionized.

Selective two-step ionization of atoms by laser radiation is now regarded as a universal method for isotope separation, for producing ultrapure materials, and for the separation of atoms containing isomeric nuclei.^[3] The method has been used to separate the isotopes of uranium,^[4] calcium,^[5] and magnesium.^[6] However, the last three papers were concerned only with the possibility of separating isotopes by two-step ionization by laser radiation, and the ion densities produced by this selective process did not exceed 10^6 cm^{-3} .

In a practical application of the process, on the other hand, one must produce high densities of selectively generated ions ($10^{12} - 10^{14} \text{ cm}^{-3}$). Resonance charge exchange with typical cross sections in the range $10^{-14} - 10^{-15} \text{ cm}^2$ ^[7] imposes an essential restriction on the upper limit of possible densities. Moreover, the process must be carried out so that each atom of the selected type is ionized, and each selectively produced ion is removed from plasma. We have succeeded, for the first time, in using the selective interaction between laser radiation and rubidium atoms to produce plasma with a density of 10^{13} cm^{-3} . The extraction of ions produced in this way by an electric field has been investigated. Every excited atom in the volume under investigation was ionized, i.e., intensity saturation was achieved for the second step.

Before the method of selective two-step ionization of atoms by laser radiation can be used, one must know the cross sections for the photoexcitation and photoionization of atoms from excited states. The photoionization cross sections are well known,^[8] but the cross sections for photoionization from excited states are practically unknown.^[9] Whenever such measurements have been performed,^[10,11] they required a knowledge of the absolute number of excited atoms, and this was difficult to determine. In this paper, we propose a simple method of measuring the cross sections for photoionization from excited states, which is based